Table S1. Block copolymer-MNPs before and after conjugation of α-chymotrypsin (ChT)

Sample	D_{eff}, nm[a]	PDI[a]	ς-potential, mV[a]	Protein : Fe ratio[b]	Modified amino groups[c]	Residual activity,% [d]
PEG-PAA/MNP	194.4 ± 4.3	0.27 ± 0.031	-70.4 ± 1.72	n.a.	n.a.	n.a.
ChT/PEG-PAA/MNP-1	147.0 ± 3.1	0.26 ± 0.006	-43.2 ± 0.41	0.13	14.0	16.3
ChT/PEG-PAA/MNP-2	122.5 ± 1.16	0.25 ± 0.001	-43.6 ± 3.54	3.94	14.0	30.7
B-GaL/PEG-PAA/MNP-2	77.8 ± 3.18	0.39 ± 0.016	-45.9 ± 2.56	1.04	n.a.	44.1
PEG-PMA/MNP	39.1 ± 1.3	0.26 ± 0.051	-48.9 ± 3.78	n.a.	n.a.	n.a.
ChT/PEG-PMA/MNP -1	56.7 ± 2.9	0.33 ± 0.019	-29.2 ± 3.08	0.27	1.6	70.9
ChT/PEG-PMA/MNP-2	55.2 ± 1.1	0.29 ± 0.037	-40.4 ± 3.71	5.3	12.8	37.7
ChT/PEG-PMA/MNP-3	44.8 ± 1.2	0.19 ± 0.025	-39.1 ± 5.91	0.54	15	29.4

[a] Intensity-mean z-averaged particle diameter (Deff), polydispersity index (PDI), and ζ-potential were measured using a Zetasizer Nano ZS 180 (Malvern Instruments Ltd., MA). [b]Weight ratio protein:Fe in the samples was varied by changing the amount of α-chymotrypsin used for conjugation. [c] As determined by TNBS titration, there are a total of 15 amino groups on α-chymotrypsin that can react with TNBS. [d] Compared to the activity of the free enzyme. Generally, the residual activity decreased as the number of enzyme attachment points (number of modified amino groups) increased.

Table S2. Residual activity (V/Vo) of free ChT and a non-conjugated ChT-MNP mixture after 3 x 2.5 min sample exposures to a 50 Hz, 110 kA/m magnetic field.

Sample	V/Vo
Free ChT	0.98± 0.13
ChT/PEG-PMA/MNP mixture	0.96± 0.21

Figure S1: Effects of Alternating Current AC magnetic field on enzyme activity

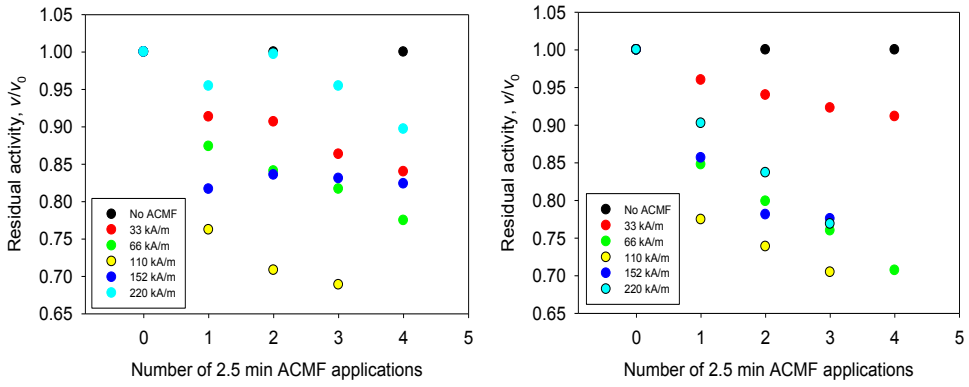

Figure S1. Changes in the residual activity (V/V_o) of α-chymotrypsin immobilized on (left) PEG-PAA/MNP (sample ChT/PEG-PAA/MNP-2) and (right) PEG-PMA/MNP (sample ChT/PEG-PMA/MNP-2) as a function of

the number of consecutive 2.5 min pulses of a 50 Hz magnetic field of different strengths. Temperature: 20 ^{o}C (± 0.1^{o}C). V_o: hydrolysis rate without exposure to the field.

Figure S2: Effect of pulsed versus continuous application of Alternating Current AC magnetic field on enzyme activity

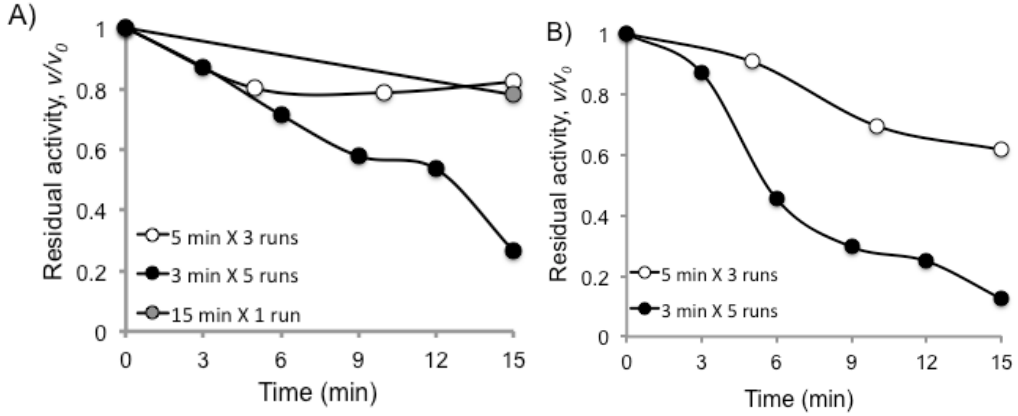

Figure S2. Effect of the RF magnetic field (337 kHz, 21 kA/m) on residual activity, V/V_o, of ChT immobilized on (A) PEG-PMA/MNP (sample ChT/PEG-PMA/MNP-3) and (B) PEG-PAA/MNP (sample ChT/PEG-PAA/MNP-1). The samples were exposed to 5 x 3 min, 3 x 5 min, or 1 x 15 min pulses of RF. V_o: hydrolysis rate without exposure to the field. Similar pulse dependence patterns were observed in Figure 2, but the inactivation effect here increased as the number of ChT molecules attached to the MNP template (enzyme/Fe weight ratio) decreased from 3.94 mg/mg (sample ChT/PEG-PAA/MNP-2, Figure 2A) to 0.54 mg/mg (sample ChT/PEG-PMA/MNP-3 (A)) or 0.13 mg/mg (sample ChT/PEG-PAA/MNP-1 (B)).

Figure S3. Effect of the solution temperature on the activity and stability of ChT-MNP aggregates:

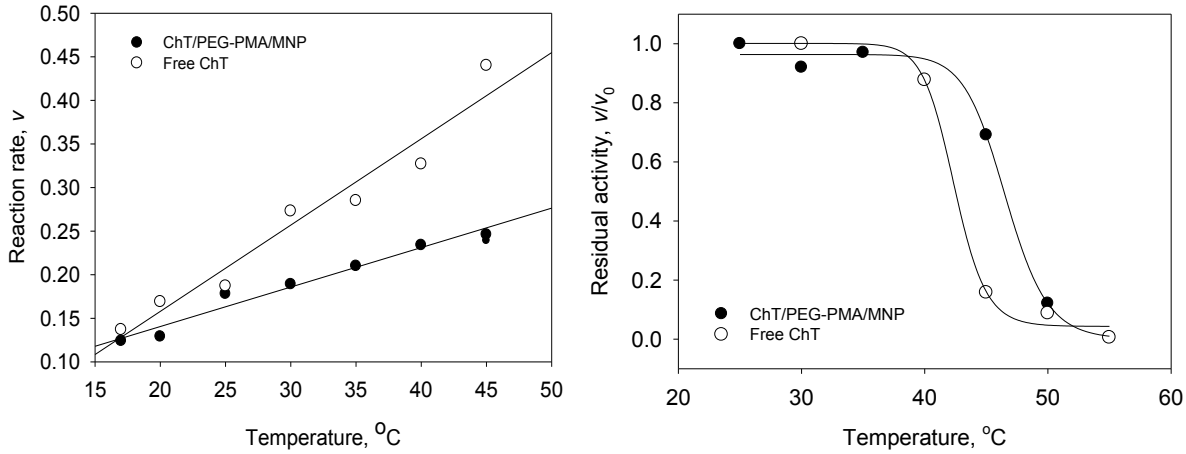

Figure S3. (Left) Dependence of the initial rate of BTNA hydrolysis (V) by free ChT and ChT immobilized on

PEG-PAA/MNP (sample ChT/PEG-PAA/MNP-2) on the temperature. (Right) Residual activity (V/V_0) of the free ChT and ChT/PEG-PAA/MNP (sample ChT/PEG-PAA/MNP-2) measured at 25°C after 5 min incubation at different temperatures. V_o: hydrolysis rate measured at 25°C before exposure to different temperatures.

2. Estimates of the surface temperature heating and surrounding considerations:

7.1. Single nanoparticle

The following model is considered: a spherical MNP is placed in the medium with given thermal properties (water) and initial temperature equal to zero. At time zero the heat release begins at a constant Specific Absorption Rate (SAR). The heat is transferred by thermal conductivity and the process is described by a Fourier differential equation in partial derivatives. Assuming that surrounding space is infinite the solution of the equation with such border conditions is presented by the following function:

$$T(r,t) = (SAR)\kappa\rho \bullet R_0^3/(3\bullet\lambda\bullet r)*(\mathrm{erfc}((r-R_0)/(2(\kappa\bullet t)^{1/2})) - \exp(r/R_0 - 1 + \kappa\bullet t/R_0^2) \bullet \mathrm{erfc}((r-R_0)/(2(\kappa\bullet t)^{1/2}) + (\kappa\bullet t)^{1/2}/R_0)) ,$$

where erfc is the supplemental integral of probabilities

$$\mathrm{erfc}(x) = \frac{2}{\pi^{1/2}} \bullet \int_x^{\infty} \exp(-y^2) dy ,$$

ρ - is the magnetite density (5,000 kg/m^3), R_0 is the radius of a MNP (10^{-8} m), λ is the thermal conductivity of the medium (0.6 W•m^{-1} K^{-1}), c is the heat capacity, $\kappa = \lambda/\rho c$ is the thermal diffusivity coefficient (≈ 1.5 •10^{-7} m^{2}s^{-1}).

This function describes the distribution of the front of the heat wave in the medium. Notably, the temperature at sufficient distance ahead of the front approximates the initial temperature. In contrast the temperature at sufficient distance behind the front approximates the stationary solution T(r) ~ 1/r.

The first summand in the equation provides for the major contribution to the heat front according to the law r ~ t$^{1/2}$. The second summand for the time intervals from 1 μs to 1,000 s and distances less than several cm provides for the minor contribution (less than 1 %), since the characteristic thermal time $\tau_0 = R_0^2/\kappa$ is less than 10^{-9} s.

Therefore, at a time scale of several ns the excess temperature at the surface of the MNP reaches a stationary value: $T(R_0) = (SAR) \bullet\rho\bullet R_0^2/(3\bullet\lambda) \approx 2.5\bullet10^{-8}$ K (assuming a typical SAR value of 10^5 W/kg[2a]). Notably, this value presents an upper estimate for the MNP surface temperatures since for the super low frequency fields used in the study, e.g. 50 Hz, the SAR values should not exceed 10^3 W/kg. The heat wave reaches the radius of the vial, ~ 5 mm, during ~ 150 s (which is comparable to the field exposure times used in our experiments). The contributions of additional heat transfer mechanisms (convection, mixing) could only increase the effective coefficient of heat transfer, which reinforces the use of this model for an upper estimate of surface temperature. This estimate is consistent with published data. For example, a precise solution of Fourier equations suggests that increase in the local temperature upon electromagnetic hyperthermia is negligible (Giordano, M.A.; Gutierrez, G.; Rinaldi, C. Int. J. Hyperthermia. **2010**, *25*, 475-484.).

2.2. Nanoparticle aggregate

Consider a single spherical aggregate comprising *N* nanoparticles (MNPs) releasing heat and placed in an infinite medium. Assuming that the heat release is uniform throughout the volume of the aggregate and the aggregate is homogeneous, the heat problem T(r, t) has a precise solution. The maximal temperature will be established in the center of the aggregate. At infinite times it will be expressed as follows:

$$T(0,+\infty) = 2\pi R_0 R_a^2 N T_0 / (4/3\pi R^3) = 1.5 N T_0 R_0/R_a = 3.75\bullet(10^{-8}\ldots10^{-6}) \text{ K},$$

where R_0 is the radius of the MNP (= 10 nm), R_a is the radius of the aggregate (100 nm), *N* is the number of MNPs in the aggregate (=10 to 1000). This estimate suggests that even at the highest possible numbers of MNPs in the aggregate (N = 1000), which exceeds by 10 to 100 fold the actual number of MNPs in the aggregates in our study, the local temperature increase in the aggregate would be negligible.

2.3. Experimental estimates

Experimental studies were also carried out to estimate temperature increases at the surface of various nanoparticles. For example, one study suggested that surface temperature may in fact increase based on measurements of fluorescence intensity of a probe immobilized at the surface of manganese ferrite ($MnFe_2O_4$) MNPs via streptavidin binding (Huang, H.; Delikanli, S.; Zeng, H.; Ferkey, D.M., Pralle, A. Nat. Nanotech. **2010**, *5*, 602-606). Notably, the fields used in this study were 40 MHz and 0.67 and 1 kA/m, and thus the product of the intensity of the magnetic field and field frequency exceeded the threshold of 4.85×10^8 A m^{-1} s^{-1}, which is considered safe and avoids significant eddy current heating in healthy tissue (A. Brezovich, Medical Physics Monograph, AIP, New York, 1988, Vol. 16, p. 82.). Moreover, the use of fluorescence intensity as a readout was challenging since this parameter is extremely sensitive to environmental effects including conformation changes and even probe dissociation that could be caused by mechanochemical forces. Other measurements involved studies upon RF heating of fluorescence peak maxima shifts of quantum dots immobilized on magnetite and gold nanoparticles, which is less sensitive to environmental effects and more robust (Gupta, A.; Kane, R.S.; Borca-Tasciuc, D.A. J. Appl. Phys. **2010**, *108*, 064901-7). A much lower frequency range (less than 1 MHz and at 0.47 kA/m) was chosen to avoid dielectric heating of the water. In this study no changes in the peak position of the immobilized vs. bulk quantum dots were observed upon RF heating, which is consistent with no or negligible changes in surface temperature as per the theoretical predictions.

3. Experimental details:

Synthesis of block ionomer stabilized magnetic nanoparticles: the MNPs were prepared as previously described[3]. $Fe(acac)_3$ (2.14 g, 8.4 mmol) and benzyl alcohol (45 mL, 0.43 mol) were charged to a 250-mL, three-neck, round-bottom flask equipped with a water condenser and placed in a Belmont metal bath with an overhead stirrer with thermostatic (± 1°C) control. The solution was dehydrated at 110°C for 1 h under a N_2 stream. The reaction was conducted with constant stirring (400-500 rpm). The temperature was increased in 25°C increments and held at each step temperature for 1 h, until it reached the reflux temperature of benzyl alcohol at 205°C, then the temperature was maintained for 40 h. The reaction was cooled to room temperature (RT) and the Fe_3O_4 particles were collected by centrifugation (4000 rpm, 30 min). The Fe_3O_4 nanoparticles were washed 3 times with acetone (100 mL each), then were dispersed in chloroform (20 mL) containing oleic acid (0.3 g) and the mixture was sonicated for ~5 min. The solvent was removed under vacuum at RT, and the oleic acid-stabilized Fe_3O_4 nanoparticles were washed 3 times with acetone (50 mL each) to remove any unbound oleic acid. The oleic acid-coated particles were dried under vacuum overnight at RT.

MNPs were coated by ligand exchange with PEG-PAA or PEG-PMA. Their average block lengths (polymerization degrees) were: 2 kDa (32) PEG and 7.2 kDa (100) PAA in PEG-PAA; and 5 kDa (80) PEG and 5.5 kDa (60) PMA in PEG-PMA. Ligand adsorption from a homogeneous organic solvent mixture was employed to assemble the block copolymers onto the MNP. Oleic acid-stabilized MNPs (50.0 mg) were dispersed in chloroform (10 mL) and charged to a 50-mL round-bottom flask. PEG-PAA (100.0 mg) was dissolved in DMF (10 mL) and added dropwise to the dispersion. The mixture was sonicated in a VWR 75T sonicator for 4 h under N_2, and then stirred at RT for 24 h. The nanoparticles were precipitated in hexane (200 mL). A permanent magnet was utilized to collect the magnetite nanoparticles and free oleic acid was decanted with the supernatant. The particles were dried under vacuum overnight at RT, then dispersed in DI water (20 mL) with adjustment of the pH to ~ 7 with 1 N NaOH and sonicated for 30 min. The particles were dialyzed against DI water (1 L) for 24 h in a 25,000 g mol^{-1} MWCO dialysis bag to remove any free polymer. The dispersion was filtered through a 0.2 μm Teflon™ filter to sterilize and to remove any large aggregates. A black-brown solid product was obtained after freeze-drying. The Fe_3O_4 the content in the samples was determined by thermogravimetric analysis (Q50, TA Instruments) of ca. 10-15 mg samples (heating 10°C/min to 110°C, isothermal for 15 min, heating 10°C/min to 700°C). SQuID magnetometry for the PEG-PAA MNPs showed a saturation magnetization of 53 emu/g of magnetite at 70,000 Oe.

Synthesis of L-cysteine (L-Cys) stabilized magnetic core-gold shell MNPs: MNP's were synthesized by co-precipitation of Fe(II) and Fe(III) chlorides in an aqueous medium. Briefly, 4 mL of 1 M aqueous $FeCl_3$ and 1 mL of 2M $FeCl_2$, each in 2 M HCl, were mixed, then added into 50 mL of 0.7 M aqueous NH_3 and kept for 30 min with stirring. The precipitate was isolated by magnetic decantation and re-dispersed in 50 mL of 2 M $HClO_4$. The Fe_3O_4 MNPs were isolated by centrifugation and re-dispersed in 50 mL of doubly-distilled water. Then, 8 mL of this

dispersion was mixed with 120 mL of a solution of $HAuCl_4$ in doublye-distilled water (0.25 mg/mL). The mixture was heated to boiling and supplemented with 5 ml 80 mM sodium citrate under constant stirring. The mixture was maintained under reflux conditions for an additional 15 min after its color changed from brown to burgundy. This solution was then mixed with 0.25 g of L-Cys, the color changed to deep blue, and the mixture was refluxed for 30 min. Finally, the L-Cys modified MNPs were centrifuged, washed with water, isolated by magnetic decantation and redispersed in 5 mL of doubly-distilled water.

Immobilization of ChT or β-GaL on block copolymer-MNP aggregates**:** PEG-PAA/MNPs or PEG-PMA/MNPs (2.5 mg) were dispersed in 0.35 mL of doubly-distilled water via sonication for 45 min. ChT or β-GaL (desired amount) was dissolved in 0.1 mL of doubly-distilled water (pH 6.5) and added to the polymer/MNP dispersion. The mixture was cooled to 4^{o}C and maintained at that temperature for 1 h, then ethyl-3-(3-dimethylaminopropyl)-carbodiimide (EDC, 2.5 mg) and 50 µL of a solution of N-hydroxysulfosuccinimide (S-NHS) (40 mg/mL in water) were added and then incubated for an additional 3 h at 4°C. Any unbound enzyme was removed by centrifugal filtration at 1,500 rpm through a 100-kDa cutoff filter, the solids were washed with phosphate buffered saline (PBS, 3 x 4 mL) and then they were dispersed in 0.5 mL of 20 mM citrate buffer, pH 5.0 for ChT or doubly-distilled water for β-Gal. The number of reacted amine groups was determined by difference by titrating residual amine groups on the bound protein with 2,4,6-trinitrobenzenesulfonic acid (TNBS)[14].

Immobilization of ChT on gold coated-MNPs: One mg of ChT was mixed with a dispersion of L-Cys modified MNPs (19 mg/ml) in doubly-distilled water, pH 5.5. The mixture was cooled to 4^{o}C for 1 h, and maintained at that temperature for 1 h, supplemented with 0.5 mg ethyl-3-(3-dimethylaminopropyl)-carbodiimide (EDC) and 25 µL of a solution of N-hydroxysulfosuccinimide (S-NHS, 4 mg/mL in water) and then incubated for an additional 2 h at 4^{o}C. The ChT modified particles were purified and re-dispersed as described previously.

The effective mobility and ζ-average hydrodynamic diameters of the block copolymer-MNPs before and after conjugation of the enzyme were measured by dynamic light scattering using a Zetasizer Nano ZS (Malvern Instruments Ltd, MA) equipped with a 633-nm laser. Scattered light was detected at 173° and 25°C. Software provided by the manufacturer which employs cumulants analysis and non-negatively constrained least-squares particle size distribution analysis was used to determine the intensity-mean ζ-average particle diameter (D_{eff}), polydispersity index (PDI), and ζ-potential. For DLS analysis, the pre-lyophilized complexes were dispersed in DI water at a concentration of 0.01 mg/mL. Mean values (intensity average diameter) were calculated from measurements conducted at least in triplicate and expressed as a mean ± standard deviation (SD).

Protein concentration in the MNPs was determined with a micro-BCA assay using ChT or β-GaL as standards.

Fe content was determined by inductively coupled plasma-mass spectrometry (ICP-MS). For ICP-MS measurements, the block copolymer-MNPs (0.01 mL) were mixed with 2 mL of 69% HNO_3 and reacted at 70^{o}C for 48 h, and then the mixture was diluted to 10 mL with distilled water.

Activity of free or conjugated ChT was determined by UV-Vis spectrometry by measuring the rate of enzymatic hydrolysis of a specific substrate, N-benzoyl-L-tyrosine *p*-nitroanilide (BTNA). Briefly, 1-2 µL of BTNA solution (17 mg/mL) in a dioxane-acetonitrile mixture (1:1 v:v) were added to 1 mL of 20 mM Tris-HCl buffer, pH 8.2, and then this was mixed with 2 µL of the free or immobilized enzyme solutions. Formation of the product (*p*-nitroaniline) was recorded at 380 nm over time. To calculate the residual activity, the activity of immobilized enzyme was calculated and compared to a standard curve of free enzyme activity. The enzymatic hydrolysis measurements followed Michaelis-Menten kinetics, showing a linear dependence on enzyme concentration and hyperbolic dependence on substrate concentration. Substrate concentrations were adjusted to maintain constant hydrolysis rates for time periods required for AC field exposures (approximately 1 h).

Activity of free or conjugated β-GaL was determined by in-situ fluorescence spectrometry with 365/445 excitation and emission values (GO!FOTON, Somerset, NJ) by measuring the rate of hydrolysis of a specific substrate, 4-Methylumbelliferyl β–D- galactopyronoside (MBDGAP). Briefly, 5 µl MBDGAP solution in 1:1 pyridine: doubly-distilled water (12 mg/ml) were added to 1.475 ml of 20 mM acetate buffer, pH 5.75 and mixed with 20 µl of a diluted nanoparticle solution (5 µl in 3.5 ml of 20 mM acetate buffer, pH 5.75). Changes in fluorescence intensity were monitored over time.